N-myc alters the fate of preneoplastic cells in a mouse model of medulloblastoma

Jessica D. Kessler,[1] Hiroshi Hasegawa,[2] Sonja N. Brun,[1] Zeng-Jie Yang,[1] John W. Dutton,[1] Fan Wang,[2] and Robert J. Wechsler-Reya[1,3]

[1]Department of Pharmacology and Cancer Biology, Duke University Medical Center, Durham, North Carolina 27710, USA; [2]Department of Cell Biology, Duke University Medical Center, Durham, North Carolina 27710, USA

Studying the early stages of cancer can provide important insight into the molecular basis of the disease. We identified a preneoplastic stage in the *patched* (*ptc*) mutant mouse, a model for the brain tumor medulloblastoma. Preneoplastic cells (PNCs) are found in most *ptc* mutants during early adulthood, but only 15% of these animals develop tumors. Although PNCs are found in mice that develop tumors, the ability of PNCs to give rise to tumors has never been demonstrated directly, and the fate of cells that do not form tumors remains unknown. Using genetic fate mapping and orthotopic transplantation, we provide definitive evidence that PNCs give rise to tumors, and show that the predominant fate of PNCs that do not form tumors is differentiation. Moreover, we show that *N-myc*, a gene commonly amplified in medulloblastoma, can dramatically alter the fate of PNCs, preventing differentiation and driving progression to tumors. Importantly, N-myc allows PNCs to grow independently of hedgehog signaling, making the resulting tumors resistant to hedgehog antagonists. These studies provide the first direct evidence that PNCs can give rise to tumors, and demonstrate that identification of genetic changes that promote tumor progression is critical for designing effective therapies for cancer.

[*Keywords*: Medulloblastoma; brain tumor; preneoplastic; hedgehog; patched]

Supplemental material is available at http://www.genesdev.org.

Received November 5, 2008; revised version accepted December 8, 2008.

Tumorigenesis is a multistep process in which cells progressively accumulate changes in genes that regulate growth, survival, differentiation, and migration (Hanahan and Weinberg 2000). Studying the early stages of the disease can provide important insight into the steps involved in transformation of normal cells into tumor cells. Indeed, preneoplastic lesions have been identified in a variety of solid cancers (Levine and Ahnen 2006; Mokbel and Cutuli 2006; Montironi et al. 2007; Singh and Maitra 2007). However, in most cases, the relationship between these lesions and the corresponding end-stage tumors has not been demonstrated directly. Proving a link between preneoplastic lesions and tumors is critical if we are to base hypotheses about tumor progression on the study of these lesions.

We studied preneoplastic lesions in a model of medulloblastoma, the *patched* (*ptc*) mutant mouse. *ptc* encodes a 12-pass transmembrane protein that functions as an antagonist of the Sonic hedgehog (Shh) signaling pathway (Lum and Beachy 2004; Jia and Jiang 2006; Rohatgi and Scott 2007). Thus, deletion or mutation of *ptc* leads to constitutive activation of the pathway. Homozygous *ptc* knockouts die during embryogenesis, consistent with the critical role of Shh signaling in many aspects of development (Goodrich et al. 1997). Heterozygotes survive to adulthood with no major developmental defects, but between 3 and 6 mo of age, ~15% of these mice develop cerebellar tumors that resemble human medulloblastoma (Goodrich et al. 1997; Wetmore et al. 2000). Since a significant proportion of human medulloblastomas have activating mutations in the Shh pathway (Fogarty et al. 2005; Dellovade et al. 2006), these mice have become a valuable model for the human disease.

To gain insight into the mechanisms of tumorigenesis in $ptc^{+/-}$ mice, we focused on the early stages of cerebellar development in these animals (Oliver et al. 2005). In wild-type mice, during the first 2 wk after birth, Shh signaling promotes proliferation of granule neuron precursors (GNPs) in the external germinal layer (EGL) on the outside of the cerebellum (Dahmane and Ruiz-i-Altaba 1999; Wallace 1999; Wechsler-Reya and Scott 1999). At this stage, $ptc^{+/-}$ mice show no obvious abnormalities in cerebellar structure. However, by 3 wk of age, when all GNPs in wild-type mice have differentiated and migrated away from the surface of the cerebellum, the majority of $ptc^{+/-}$ mice still have clusters of proliferating cells on the cerebellar surface (Goodrich et al. 1997; Kim et al. 2003; Oliver et al. 2005). These ectopic cells resemble GNPs in terms of morphology and location, but differ from GNPs (and resemble tumor cells) in that they have lost expression

[3]**Corresponding author.**
E-MAIL rw.reya@duke.edu; FAX (919) 668-3556.
Article is online at http://www.genesdev.org/cgi/doi/10.1101/gad.1759909.

of the wild-type *ptc* allele (Oliver et al. 2005). Moreover, gene expression profiling suggests that these cells are readily distinguishable from both GNPs and tumor cells. Based on these observations, we postulated that they represent an intermediate stage between normal GNPs and medulloblastoma cells, and referred to them as preneoplastic cells (PNCs).

PNCs are found in 70%–80% of mice between 3 and 8 wk of age, but by 3 mo, proliferating cells are only detectable in the subset of mice that have developed, or will develop, tumors (Oliver et al. 2005). These findings raise several key questions. First, do PNCs actually give rise to tumors? The fact that they are present in animals destined to develop medulloblastoma is certainly consistent with this possibility, but it is also possible that tumors arise from a distinct population of cells (e.g., neural stem cells). Second, what is the fate of PNCs in animals that do not develop tumors? Do they simply die, or can they undergo the same pattern of differentiation and migration as normal GNPs? And finally, are the PNCs that do not form tumors irreversibly committed to their fate, or do they retain the capacity to form tumors if given the appropriate genetic stimuli?

To investigate these questions, we generated a novel reporter mouse to genetically mark PNCs in vivo. Using this mouse, we show that the majority of PNCs undergo differentiation and migrate into the internal granule layer (IGL) of the cerebellum. However, in some animals, PNCs continue to divide and ultimately give rise to tumors. A subset of PNCs can also give rise to tumors following transplantation, but overexpression of the oncogene *N-myc* dramatically increases the tumorigenic potential of these cells, allowing them to generate tumors in 100% of recipients. N-myc promotes tumorigenesis by increasing proliferation and suppressing differentiation, and in the process, renders cells resistant to hedgehog pathway antagonists. These studies indicate that PNCs represent a critical stage of tumorigenesis, during which cells have the capacity to decide whether to differentiate or whether to continue proliferating and give rise to medulloblastoma. Moreover, they suggest that acquisition of certain oncogenic mutations may not only promote tumor formation, but may determine the responsiveness of tumor cells to molecular targeted therapy.

Results

PNCs disappear from the surface of the cerebellum

Although the majority of 3- to 8-wk-old $ptc^{+/-}$ mice have PNCs in their cerebellum (Oliver et al. 2005), the fate of these cells has never been analyzed in detail. To investigate this, we crossed $ptc^{+/-}$ mice with Math1-GFP (green fluorescent protein) transgenic mice (Lumpkin et al. 2003; Oliver et al. 2005), which express GFP under the control of the *Math1* enhancer. Math1 is a transcription factor that is expressed in proliferating GNPs and is maintained in PNCs and tumor cells from $ptc^{+/-}$ mice (Ben-Arie et al. 2000; Kim et al. 2003; Lee et al. 2003; Lumpkin et al. 2003; Oliver et al. 2005). Consistent with this, we detected expression of GFP in the EGL of neonatal Math1-GFP mice (Fig. 1A), and in preneoplastic lesions and tumors in adult Math1-GFP;$ptc^{+/-}$ (M-ptc) mice (Fig. 1B,C). The M-ptc mouse allowed us to perform detailed quantitative analysis of the number and size of preneoplastic lesions at various stages. At 6 wk of age, 75% of M-ptc animals had GFP^+ lesions on the surface of their cerebellum, whereas at 12 wk, only 19% of mice had GFP^+ lesions (Fig. 1D), approximating the percentage of animals that end up developing medulloblastoma. Similar results were obtained by staining cerebella from $ptc^{+/-}$ mice with the nuclear dye DAPI, whose fluorescence (unlike Math1-GFP) is not dependent on differentiation status (Supplemental Fig. 1): At 6 wk of age, most mice had multiple large regions of DAPI staining on the surface of their cerebellum, but by 12 wk, the number and size of these lesions was much smaller. Together, these studies indicate that the majority of PNCs disappear from the surface of the cerebellum by 12 wk of age.

Preneoplastic lesions exhibit little apoptosis

In principle, the disappearance of PNCs could reflect cell death or migration away from the surface of the cerebellum.

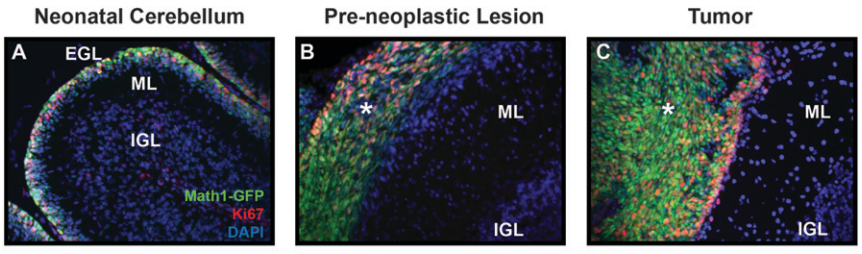

D

Age	# of mice with GFP+ lesions	% of mice with GFP+ lesions
6 weeks	12/16	75%
12 weeks	3/16	19%

Figure 1. $ptc^{+/-}$ mice have ectopic Math1-GFP^+ cells on the surface of their cerebellum. (*A–C*) Cerebellar sections from P7 Math1-GFP mice, 5- to 6-wk-old Math1-GFP/$ptc^{+/-}$ (M-ptc) mice, and tumor-bearing M-ptc mice were stained with antibodies specific for the proliferation marker Ki67 (red) and with DAPI, to label all nuclei. Sections were imaged at 20× magnification using a Leica AxioImager and Metamorph software. Note the colocalization of GFP with Ki67 in the EGL (*A*), in preneoplastic lesions (asterisk, *B*), and in tumors (asterisk, *C*). (*D*) M-ptc mice were sacrificed at either 6 or 12 wk of age and cerebella were examined for the presence of GFP^+ lesions. While the majority of M-ptc mice have GFP^+ lesions at 6 wk, most of these lesions have disappeared by 12 wk of age. (EGL) External germinal layer; (IGL) internal granule layer; (ML) molecular layer.

To determine whether apoptosis contributed to the loss of PNCs, we stained cerebellar sections from $ptc^{+/-}$ mice with antibodies specific for cleaved caspase-3 (CC-3), a marker of apoptotic cells. Whereas tumors from these animals contained significant numbers of CC-3$^+$ cells (Supplemental Fig. 2C), neonatal cerebellum and preneoplastic lesions exhibited little or no CC-3 staining (Supplemental Fig. 2A,B). Similar results were observed using terminal deoxynucleotidyl transferase dUTP nick end labeling (TUNEL) staining (Supplemental Fig. 2D–F). Although we cannot rule out the possibility that some PNCs undergo apoptosis, these data suggest that it is not the primary mechanism of PNC disappearance.

Generation of reporter mice to track the fate of PNCs

Another possible explanation for the loss of PNCs from the surface of the cerebellum was differentiation and migration. Since expression of Math1-GFP is extinguished when cells stop dividing, the M-ptc mouse cannot be used to follow the fate of PNCs that have undergone differentiation. Therefore, to track these cells, we generated a novel reporter mouse: We crossed $ptc^{+/-}$ mice with Math1-CreER transgenics, which carry a tamoxifen-inducible form of the Cre recombinase under the control of the *Math1* enhancer (Machold and Fishell 2005) and with R26R-hPLAP (human placental alkaline phosphatase [AP]) mice, which carry a loxP-flanked stop sequence upstream of the *hPLAP* gene. The triple transgenics resulting from these crosses, which we call MAP (Math1-CreER/AP/$ptc^{+/-}$) mice, allowed us to permanently label Math1-expressing cells upon treatment with tamoxifen.

To test the utility of these animals for fate mapping, we treated them with tamoxifen at postnatal day 8 (P8, to label GNPs), at 4 wk (to label PNCs), or at onset of clinical symptoms (to label tumor cells). Mice were sacrificed 3 d after tamoxifen treatment, and cerebellar sections were stained with AP substrate to detect marked cells. As shown in Figure 2, A and B, tamoxifen treatment at P8 resulted in staining of most GNPs in the EGL and a subset of mature granule neurons in the IGL (presumably derived from recently differentiated GNPs). Preneoplastic lesions (Fig. 2C,D) and tumor cells (Fig. 2E,F) could also be labeled in this manner; importantly, AP expression in adults was restricted to these cells, and no staining was seen in the surrounding normal cerebellum. Thus, MAP mice allow specific labeling of Math1$^+$ GNPs, PNCs, and tumor cells.

To determine whether labeled cells retain AP expression over longer time periods, we treated animals with tamoxifen at P8 and sacrificed them at P21. By this stage, all GNPs that were expressing Math1 at P8 should have turned off Math1 expression, differentiated, and migrated into the IGL. As expected, histological staining (Fig. 2G) revealed a molecular layer (ML) nearly devoid of cells and an IGL densely packed with granule neurons. AP staining revealed expression of the marker in a large proportion of granule neurons in the IGL (Fig. 2H). Interestingly, strong AP staining was also seen at the surface of the cerebellum; this was associated with the axons of granule neurons, which are left behind when cells migrate inward. This unique feature of the AP transgene allowed us to track not only where labeled cells went, but also where they had been.

Most PNCs undergo differentiation and migration

Having established that MAP mice could be used for long-term labeling of Math1$^+$ cells, we used these animals to track the fate of PNCs. We treated MAP mice with a single dose of tamoxifen at 4–5 wk of age (a stage at which PNCs are the only Math1$^+$ cells in the cerebellum) and harvested cerebella 3 d, 1 mo, or 2 mo later. Three days after tamoxifen treatment, preneoplastic lesions were strongly positive for both AP and the proliferation marker Ki67 (Fig. 3A,B). In addition to staining within the lesions themselves, we also observed small numbers of AP-expressing cells in the underlying IGL (Fig. 3C,D); these cells did not express Ki67, but did express the differentiation marker NeuN. Thus, even within 3 d, some PNCs exit the cell cycle and migrate into the IGL.

One month after tamoxifen treatment (Fig. 3E–H), large groups of cells could still be found on the surface of the cerebellum in many MAP mice (Fig. 3E). These cells expressed AP, but were no longer proliferating (note the lack of Ki67 staining in Fig. 3F). In addition, many cells had AP-positive processes and appeared to be migrating toward the IGL (Fig. 3F–H). Both migrating cells and cells within the primary lesion expressed NeuN (Fig. 3G,H), indicating that by this time point the majority of PNCs had undergone differentiation.

Two months after tamoxifen treatment, few cells were observed at the surface of the cerebellum (Fig. 3I). While some regions of the cerebellar surface exhibited very strong AP staining (arrows in Fig, 3J,K), these regions were largely devoid of cell bodies (arrow, Fig. 3I), and the staining appeared to represent the processes of cells that had migrated into the IGL (Fig. 3J–L). AP-labeled cells in the IGL lacked Ki67 (Fig. 3J) and expressed Gabra6, a marker associated with terminally differentiated granule neurons (Fig. 3K,L). In addition to lesions that exhibited extensive migration, we also observed a small number of PNCs that remained on the surface of the cerebellum; staining for Ki67 and NeuN revealed that these cells had ceased proliferating and undergone differentiation (data not shown). Consistent with our previous findings (Oliver et al. 2005), most PNCs, whether proliferating or differentiated, lacked expression of the wild-type allele of *ptc* (Supplemental Fig. 3). These data indicate that despite loss of *ptc*, PNCs are able to undergo differentiation and migration in a pattern similar to that exhibited by normal granule neurons.

PNCs can give rise to tumors

Although the majority of PNCs undergo differentiation and migration, a subset of these cells is presumed to persist and give rise to medulloblastoma. But while PNCs have been suggested to represent the source of tumors in $ptc^{+/-}$ mice, this has never been formally demonstrated; in fact, some investigators have suggested that tumors could arise from a distinct cell type in the adult cerebellum, such as a multipotent stem cell (Berman et al. 2002;

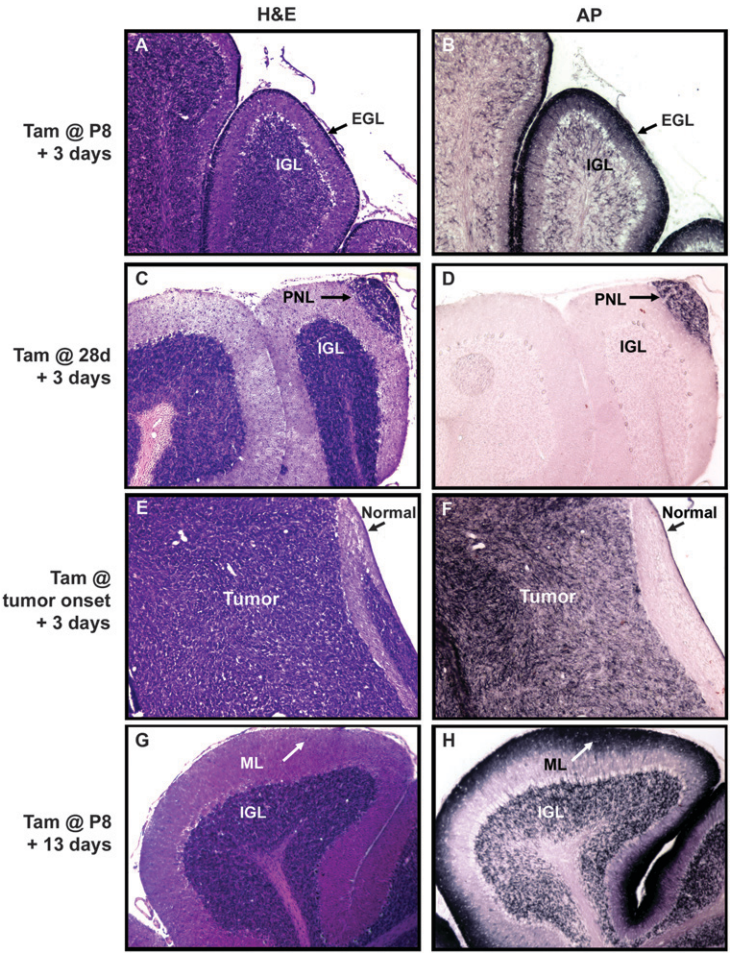

Figure 2. MAP mice can be used to label Math1$^+$ cells. Math1-CreER/AP mice were treated with a single dose of tamoxifen at P8 (*A*,*B*,*G*,*H*), and MAP mice were treated at 28 d (*C*,*D*) or when they showed symptoms of medulloblastoma (*E*,*F*). Animals were sacrificed 3 d later for short-term labeling (*A*–*F*) or 13 d later for long term labeling (*G*,*H*). Adjacent sections were stained with H&E to detect tissue morphology (*A*,*C*,*E*,*G*) or with the substrate NBT/BCIP to identify cells in which AP expression had been induced (*B*,*D*,*F*,*H*). Magnification, 10×. Note the expression of AP in the EGL (arrows in *A*,*B*), preneoplastic lesions (arrows in *C*,*D*), and tumor (*F*). (*G*,*H*) AP staining persisted in granule neurons that were exposed to tamoxifen at P8 and allowed to undergo differentiation and migration into the IGL. (*H*) Staining was also observed in the processes of these cells that remained at the surface of the cerebellum (arrow).

Hemmati et al. 2003; Li et al. 2003; Singh et al. 2004). To determine whether tumors are derived from Math1$^+$ PNCs, we treated MAP mice with tamoxifen at 5 wk of age and sacrificed them when they exhibited clinical signs of medulloblastoma. Figure 4A shows a brain from one such mouse after whole-mount staining for AP. Intense staining can be seen in the tumor, whereas the normal cerebellum and the rest of the brain are unlabeled. In sections, tumors are clearly detectable by H&E staining (Fig. 4B), and are specifically labeled with AP substrate (Fig. 4C). Among the tumors that were analyzed in these studies (n = 6), all were positive for AP. These results indicate that tumors arise from Math1$^+$ PNCs rather than from Math1$^-$ progenitors.

To further investigate the capacity of PNCs to give rise to tumors, we used an orthotopic transplantation assay. We isolated PNCs from individual *ptc*$^{+/-}$ or M-ptc mice and implanted 5×10^5 cells from each animal into the cerebellum of a SCID-beige host (Fig. 5A). As a positive control, some mice were implanted with 5×10^5 cells from established tumors. To follow the fate of transplanted cells, we stained cerebellar sections from transplant recipients with antibodies specific for β-galactosidase (βgal) (*ptc*$^{+/-}$ mice have the *βgal* gene inserted into the *ptc* locus, and therefore express the enzyme in cells that would normally express *ptc,* including GNPs, PNCs, and tumor cells and their post-mitotic derivatives) (Goodrich et al. 1997; Oliver et al. 2005).

As early as 2 wk after transplantation, *ptc*$^{+/-}$ tumor cells had formed large proliferating (βgal$^+$Ki67$^+$) masses in the cerebellum of recipients (Fig. 5C). Transplanted PNCs could also be detected at this stage (Fig. 5D); while some cells were still proliferating, many had exited the cell cycle and begun to express markers of differentiation (NeuN) (Fig. 5E). By 6–8 wk after transplantation, 100% (12 out of 12) of mice that had received tumor cells developed symptoms of medulloblastoma (Fig. 5B). In contrast, the majority of mice transplanted with PNCs did not develop symptoms; in these animals, small numbers of βgal$^+$ cells could often be found around the IGL 4 mo after transplantation (Supplemental Fig. 4). Notably, 13% (four out of 32) of animals transplanted with PNCs did develop tumors 8–11 wk post-transplantation. Since each PNC transplant was derived from a single donor, and since ~15% of donors would have developed tumors had they not been sacrificed, these results support the notion that a subset of PNCs is capable of giving rise to tumors, and demonstrate that the intrinsic tumorigenic potential of these cells is conserved in the transplantation assay.

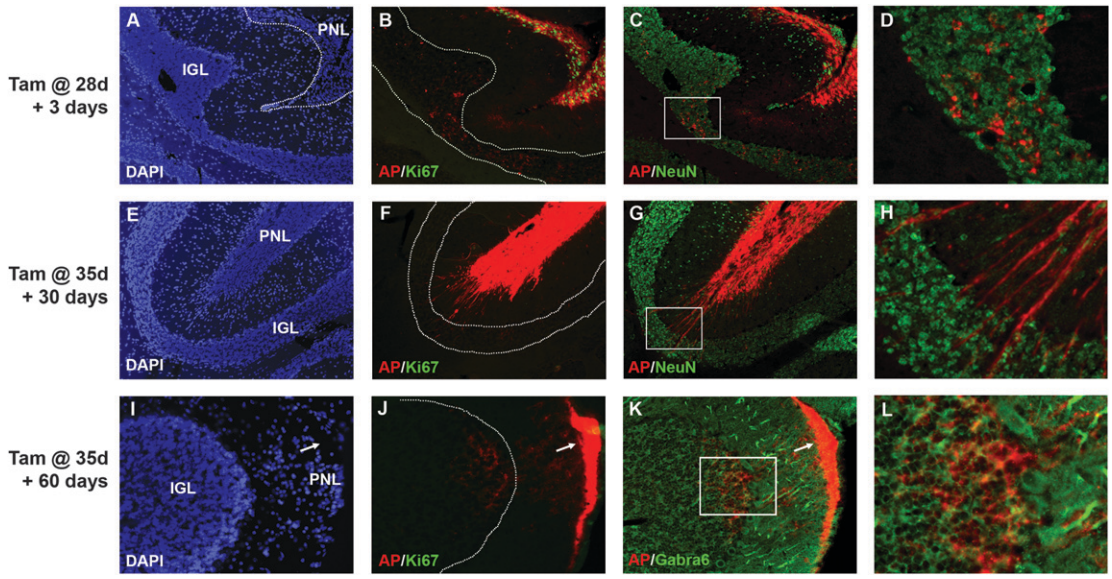

Figure 3. The majority of preneoplastic lesions undergo differentiation and migration. Four-week-old to 5-wk-old MAP mice were treated with tamoxifen for 3 d (*A–D*), 30 d (*E–H*), or 60 d (*I–L*). Sections were stained with DAPI (*A*,*E*,*I*) or with the AP substrate Fast Red and with antibodies specific for Ki67 (green in *B*,*F*,*J*), NeuN (green in *C*,*D*,*G*,*H*) or Gabra6 (green in *K*,*L*). Three days after treatment, AP-labeled PNCs within surface lesions express Ki67 (*B*), but some NeuN$^+$ cells can be seen migrating away from the surface and into the IGL (*C*,*D*). Thirty days after treatment, AP-positive cells no longer express Ki67 (*F*) and many NeuN$^+$ cells can be seen migrating into the IGL (*G*,*H*). Sixty days after treatment, few cells can be detected at the surface (*I*), but AP-labeled processes (arrows in *J*,*K*) are seen in acellular regions at the surface (arrow in *I*), and AP-labeled cells expressing the terminal differentiation marker Gabra6 can be found in the underlying IGL (*K*,*L*). Magnifications: *A–C*,*E–G*, 10×; *I–K*, 20×; *D*,*H*, 40×; *L*, 60×. Regions in *D*, *H*, and *L* correspond to boxes in *C*, *G*, and *K*, respectively.

N-myc increases the tumorigenic potential of PNCs

The fact that the majority of PNCs do not form tumors—either in their original hosts or following transplantation—suggests that these cells are not fully transformed. But whether they are already committed to differentiate, or whether they retain the capacity to give rise to tumors, is unclear. To test whether nontumorigenic PNCs can be induced to form tumors, we sought to provide them with a "second hit." We chose the *N-myc* oncogene because it has been shown to be amplified or overexpressed in human medulloblastoma (Aldosari et al. 2002; Eberhart et al. 2002; Pomeroy et al. 2002) as well as in several mouse models of the disease (Shakhova et al. 2006; Yan et al. 2006; Frappart et al. 2007; Zindy et al. 2007). We isolated PNCs from individual *ptc*$^{+/-}$ mice, infected half the cells with a control GFP retrovirus and half with an N-myc-IRES-GFP retrovirus, and then implanted cells into the cerebellum of SCID-beige hosts. This experimental design allowed us to compare the fate of control and N-myc-infected cells from the same donor.

Although a subset of animals (five out of 15) transplanted with GFP-infected cells developed tumors, the majority of animals receiving GFP-infected PNCs remained asymptomatic and exhibited normal cerebellar structure 4 mo after transplantation (Fig. 6A). Transplanted PNCs could often be detected in these animals, but they were no longer proliferating (Fig. 6B). In contrast, all animals transplanted with N-myc-infected cells developed large tumors within 3 mo of transplantation (Fig. 6C,D). Compared with tumors derived from GFP-infected PNCs, tumors derived from N-myc-infected PNCs developed much more rapidly (median latency 45 vs. 95 d) and were more invasive, often migrating

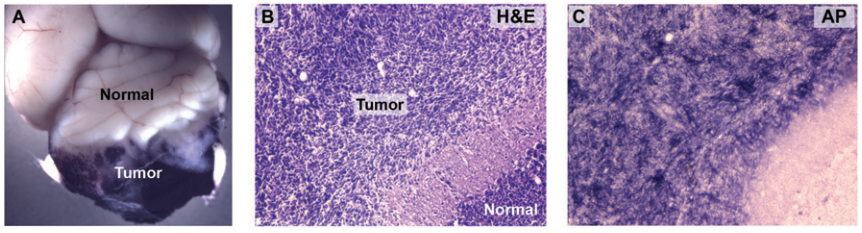

Figure 4. Preneoplastic lesions can give rise to tumors in vivo. MAP mice were treated with tamoxifen at 5–6 wk of age and sacrificed when they displayed clinical signs of medulloblastoma. (*A*) Whole-mount NBT/BCIP staining of brains from these mice showed high levels of AP only in the tumor and not in the normal cerebellum or forebrain. H&E staining (*B*) and NBT/BCIP staining (*C*) of tissue sections confirmed that tumors consisted of cells that had been induced to express AP at 5–6 wk. Magnification, 20×.

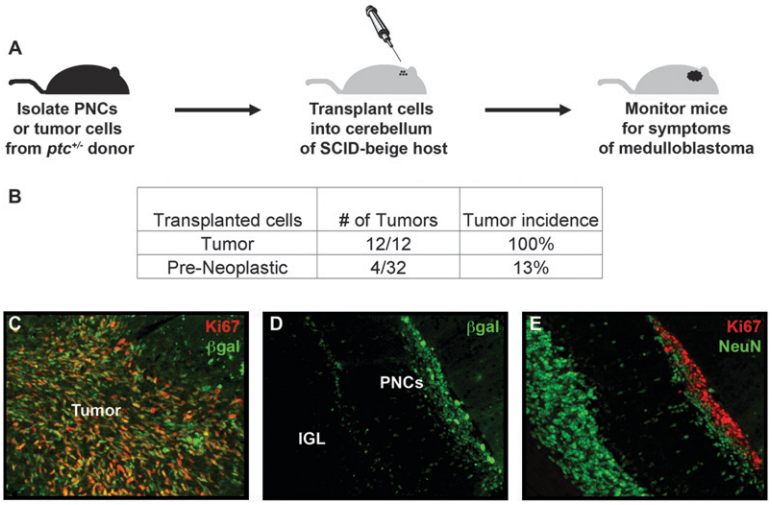

Figure 5. PNCs rarely form tumors following transplantation. (*A*) Design of orthotopic transplantation assay. We isolated 5×10^5 PNCs or tumor cells from $ptc^{+/-}$ or M-ptc mice and transplanted them into the cerebellum of SCID-beige hosts to assay for tumorigenicity. (*B*) Incidence of tumors from transplanted PNCs or tumor cells. (*C–E*) PNCs and tumor cells were transplanted as described above and hosts were sacrificed 2 wk later. Cerebellar sections were stained with antibodies specific for βgal to detect transplanted cells (*C*,*D*), Ki67 (*C*,*E*), or NeuN (*E*). (*C*) Two weeks after transplantation, βgal^+ tumor cells had formed a proliferating ($Ki67^+$) mass in the cerebellum. (*D*) βGal^+ PNCs could also be detected at this stage. (*E*) Although some of these cells were proliferating (Ki67), many had exited the cell cycle and expressed the differentiation marker NeuN. Magnification 20×.

through normal cerebellar tissue and into the forebrain (see arrow in Fig. 6C). Tumors from N-myc-infected PNCs could be propagated by transplantation into secondary hosts, indicating that they were fully transformed and not simply exhibiting prolonged proliferation. Overall, N-myc increased the tumorigenic potential of PNCs from 33% to 100% (Fig. 6E). In contrast to PNCs, wild-type GNPs infected with N-myc retroviruses did not form tumors after transplantation (data not shown). These data suggest that overexpression of N-myc can only promote tumor formation in cells that have lost *ptc* (a characteristic of PNCs but not of GNPs). In a broader sense, they show that while most PNCs are not fully transformed, given an appropriate oncogenic stimulus they have the capacity to give rise to medulloblastoma.

N-myc overexpression maintains proliferation and prevents differentiation of PNCs

Since our lineage-tracing and transplantation studies both suggested that the default fate of PNCs was differentiation, we sought to determine whether N-myc allowed PNCs to form tumors by interfering with their capacity to differentiate. Previous studies have demonstrated that GNPs and tumor cells from $ptc^{+/-}$ mice can be induced to differentiate by basic fibroblast growth factor (bFGF) (Fogarty et al. 2007). As shown in Supplemental Figure 5, PNCs also exit the cell cycle and differentiate when exposed to bFGF. To investigate the effects of N-myc on bFGF-induced differentiation, we infected cells with GFP or N-myc retroviruses and cultured them in the presence or absence of bFGF (Fig. 7A). N-myc not only increased the basal proliferation of PNCs, but also rendered cells resistant to bFGF-induced differentiation.

To understand the mechanisms by which N-myc exerted its effects, we FACS sorted control and N-myc-infected cells and analyzed their expression of hedgehog target genes and markers of proliferation and differentiation. As shown in Figure 7, B–D, (gray bars), GFP-infected PNCs expressed low levels of *gli1* (a direct target of the hedgehog pathway), *cyclin D1* (a marker of cell cycle progression), and *math1* (a marker of undifferentiated cells). In contrast, N-myc-infected PNCs showed elevated levels of these genes, suggesting that it was capable of maintaining proliferation and preventing differentiation.

The fact that N-myc induced expression of *gli1* raised the possibility that it might be preventing differentiation simply by maintaining hedgehog pathway activity. To determine whether the effects of N-myc were dependent on the hedgehog pathway, we treated control and N-myc-infected cells with cyclopamine (Fig. 7B–D, black bars). In GFP-infected PNCs, cyclopamine reduced expression of *gli1*, *cyclin D1*, and *math1*, indicating that in these cells hedgehog signaling was required for continued proliferation and maintenance of the undifferentiated state. In N-myc-infected cells, cyclopamine abrogated expression of *gli1*, but had little effect on expression of cyclin D1 and Math1. Thus, N-myc allowed PNCs to maintain proliferation and resist differentiation even in the absence of continued hedgehog signaling.

Previous studies have shown that N-myc can regulate proliferation and differentiation by controlling the levels of the cyclin-dependent kinase inhibitor $p27^{Kip1}$ (Nakamura et al. 2003; Zindy et al. 2006). To determine whether N-myc affected p27 expression in PNCs, we infected cells with control or N-myc retroviruses and then stained them with antibodies specific for p27 (Fig. 7E–I). After 48 h in culture, approximately half of control PNCs expressed p27 (Fig. 7E), whereas only 25% of N-myc-infected cells were $p27^+$ (Fig. 7F). Notably, cyclopamine treatment markedly increased expression of p27 in control cells (to 80%) (Fig. 7G), whereas it had little effect on p27 expression in N-myc infected cells (30% $p27^+$) (Fig. 7H). Together these data suggest that N-myc may prevent PNCs from exiting the cell cycle and differentiating by inducing expression of cyclin D1 and suppressing expression of p27. Moreover, since the effects of N-myc are not blocked by cyclopamine, they suggest that N-myc can sustain proliferation and prevent differentiation of PNCs even in the absence of hedgehog signaling.

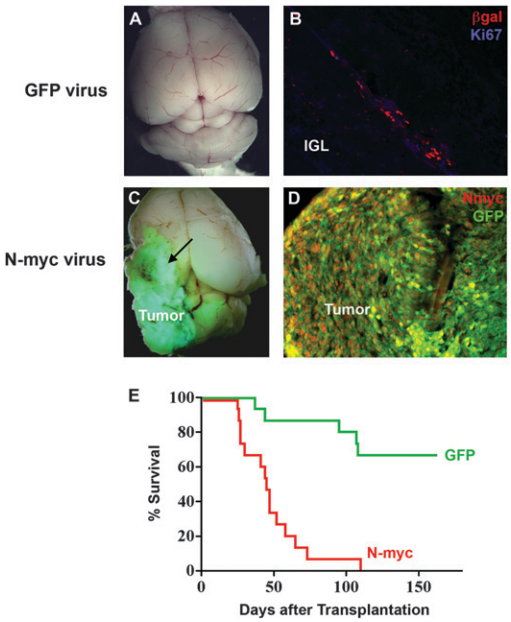

Figure 6. N-myc overexpression increases the tumorigenic potential of PNCs. PNCs were isolated from 5- to 6-wk-old $ptc^{+/-}$ mice and infected with either control GFP virus or N-myc-IRES-GFP virus. After 24 h, 5×10^5 cells were implanted into the cerebellum of SCID-beige hosts. (*A*) Whole-mount imaging of a host brain transplanted with GFP-infected PNCs showed normal morphology 4 mo after transplantation. (*B*) Section from the animal shown in *A*, stained with anti-βgal (red) and anti-Ki67 (blue) antibodies. Transplanted PNCs could be located by βgal staining, but were not proliferating. (The faint blue staining is not nuclear and is also seen with isotype-control antibodies, and is therefore nonspecific.) (*C*) Whole-mount imaging of a host brain transplanted with N-myc-infected PNCs, showing the large GFP^+ tumors that result from such transplants. Tumors from N-myc-infected PNCs, unlike those from control PNCs, frequently invade the forebrain (arrow). (*D*) Section from the animal shown in *C*, stained with antibodies specific for N-myc (red) and GFP (green). Magnification in *B* and *D* is 20×. (*E*) Survival of mice receiving GFP-infected and N-myc-infected PNCs, showing the increased incidence and decreased latency of tumors arising from N-myc-infected PNCs.

N-myc renders tumors resistant to hedgehog antagonists

Since N-myc rendered PNCs resistant to the inhibitory effects of hedgehog antagonists in vitro, we wondered whether it would have the same effect in the context of tumor formation. To test this, we infected PNCs with N-myc viruses and then cultured them for 24 h in medium lacking or containing cyclopamine before transplanting them into the cerebellum of SCID-Beige hosts. As expected, all animals ($n = 4$) transplanted with N-myc-infected PNCs developed tumors. Strikingly, all animals ($n = 4$) receiving cyclopamine-pretreated cells also developed tumors, and cyclopamine had no effect on latency, mitotic index, or invasiveness (Fig. 8A,B). In contrast, cyclopamine and other hedgehog antagonists potently suppress the growth of conventional $ptc^{+/-}$ tumor cells (Berman et al. 2002; Sanchez and Ruiz i Altaba 2005; Sasai et al. 2006; data not shown). Thus, N-myc allows PNCs to form tumors despite inhibition of hedgehog signaling.

To determine whether tumors arising from N-myc-infected PNCs remain resistant to hedgehog antagonists once they are established, we isolated tumor cells from hosts after they had developed clinical signs of medulloblastoma and treated them with cyclopamine or bFGF. In contrast to tumor cells from $ptc^{+/-}$ mice, which exhibit almost complete growth inhibition by these agents (Fig. 8C; Fogarty et al. 2007), tumor cells derived from N-myc-infected PNCs showed minimal inhibition by these agents (Fig. 8D). These data indicate that N-myc not only promotes transformation of PNCs, but in the process, renders cells resistant to hedgehog antagonists. Although such antagonists have shown promise in preclinical studies (Romer and Curran 2005) and are currently moving toward clinical trials (Epstein 2008), our studies raise the possibility that tumors that are initially dependent on the hedgehog pathway may acquire secondary mutations that render them insensitive to these agents.

Discussion

Studying the early stages of cancer can provide important insight into the steps involved in transformation. In the studies described above, we use genetic fate-mapping and orthotopic transplantation to determine the fate of PNCs in a mouse model of medulloblastoma. We show that the majority of PNCs undergo differentiation, but that a subset of these cells goes on to form tumors. Notably, PNCs that do not normally form tumors are not irreversibly committed to differentiate. Rather, given an appropriate oncogenic mutation, these cells retain the capacity to become transformed and give rise to tumors. We also show that the nature of this mutation is critical: N-myc not only promotes tumor progression but also renders cells resistant to hedgehog antagonists. These studies provide definitive evidence that tumors in $ptc^{+/-}$ mice arise from PNCs and identify the preneoplastic stage as a key decision point at which cells have the capacity to choose whether or not to progress to malignancy. Moreover, they demonstrate that genetic changes that occur at the preneoplastic stage may be critical determinants of tumor progression as well as responsiveness to therapy.

Preneoplastic lesions have been described in $ptc^{+/-}$ mice (Goodrich et al. 1997; Kim et al. 2003; Oliver et al. 2005) and in other models of medulloblastoma (Hallahan et al. 2004; Uziel et al. 2005), but the long-term fate of these lesions has not been investigated in detail. In part, this is due to limitations in the tools that have been available to study them. For example, while the Math1-GFP transgene in M-ptc mice can be used to identify PNCs while they are proliferating, (Goodrich et al. 1997; Oliver et al. 2005), expression of GFP is lost as soon as PNCs exit the cell cycle and differentiate. In contrast, the *βgal* gene (which is knocked into the *ptc* locus in $ptc^{+/-}$ mice) is expressed in PNCs as well as in post-mitotic granule neurons, so βgal^+ PNCs that have migrated into

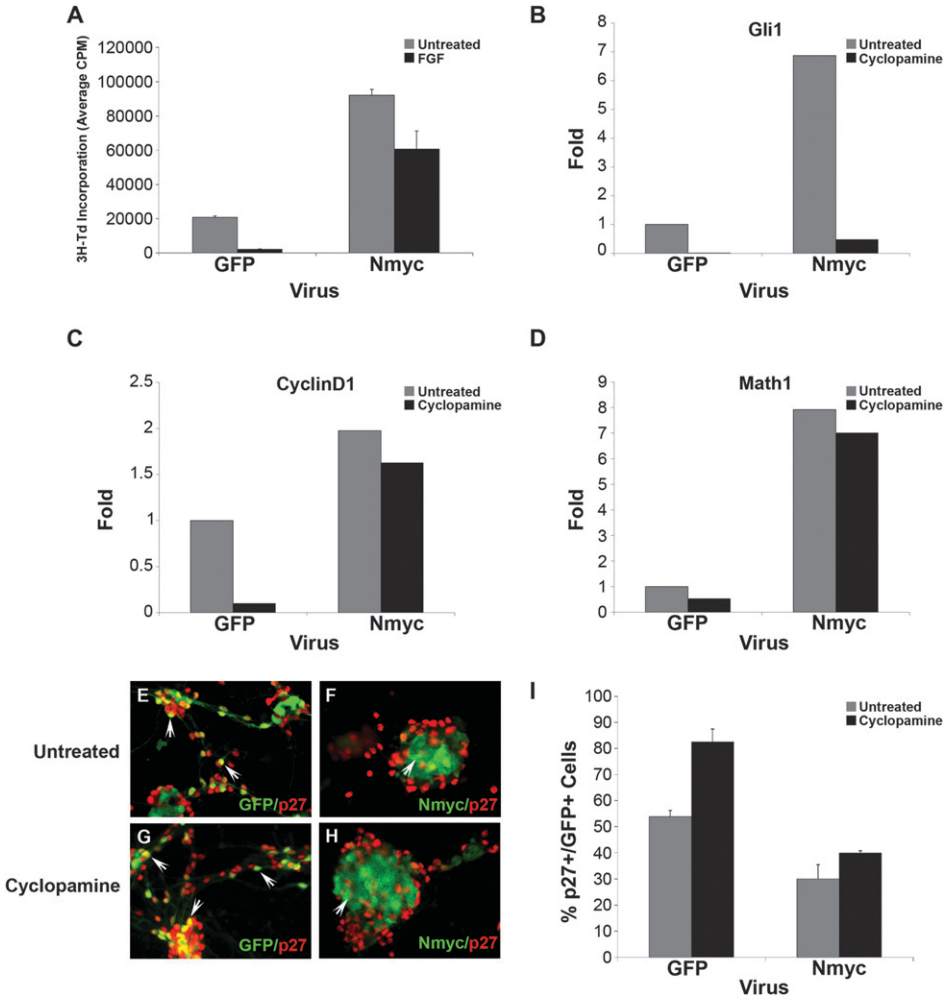

Figure 7. N-myc promotes proliferation and prevents differentiation of PNCs. (*A*) PNCs were infected with either GFP or N-myc retroviruses and then cultured for 48 h in the absence (untreated) or presence of 25 ng/mL bFGF before being pulsed with tritiated thymidine (^{3}H-Td). Although bFGF inhibited proliferation of GFP-infected cells, little inhibition was seen in cells infected with N-myc viruses. (*B–D*) PNCs were infected with either GFP or N-myc retroviruses and then cultured for 48 h in the absence or presence of 1 μM cyclopamine. Infected (GFP$^+$) cells were FACS-sorted and RNA was isolated and analyzed by real-time RT–PCR using primers specific for *Gli1* (*B*), *CyclinD1* (*C*), or *Math1* (*D*); data are representative of three replicate experiments. (*E–H*) PNCs cultured in PDL-coated chamber slides were infected and treated with cyclopamine as described above. Infected cells were stained with anti-p27 antibodies and imaged using a Leica AxioImager and Metamorph software. (*I*) Data from experiments in E-H were quantitated by counting the number of p27$^+$/GFP$^+$ cells (averaged from four fields per well). These data are representative of five individual replicates of the experiment.

the IGL are indistinguishable from surrounding cells. To overcome these limitations, we developed the MAP reporter mouse, which allowed us to permanently label PNCs with AP. Using this mouse we were able to demonstrate that after a period of prolonged proliferation, the majority of PNCs undergo differentiation and migrate into the IGL.

The ability of PNCs to undergo differentiation is significant in light of our findings (Supplemental Fig. 3; Oliver et al. 2005) that the majority of these cells no longer express the wild-type allele of *ptc*. This implies that loss of *ptc*—and the constitutive hedgehog pathway activation that results from it—is not sufficient to keep cells from exiting the cell cycle and differentiating. Several factors have been shown to be capable of overcoming Shh-induced proliferation and promoting differentiation of GNPs (Nicot et al. 2002; Fogarty et al. 2007; Zhao et al. 2008); it is possible that these factors contribute to differentiation of PNCs as well. It is also notable that PNCs are able to execute a relatively normal program of differentiation and migration in the adult cerebellum, a microenvironment that is quite different from the one in which GNPs normally differentiate. One interpretation of this is that PNCs are capable of creating or maintaining a microenvironment that resembles the neonatal cerebellum, thereby preserving the exogenous cues that allow them to differentiate and migrate. Alternatively, it is possible that the signals necessary for differentiation and migration are intrinsic to PNCs themselves. The fact that these cells are also capable of surviving

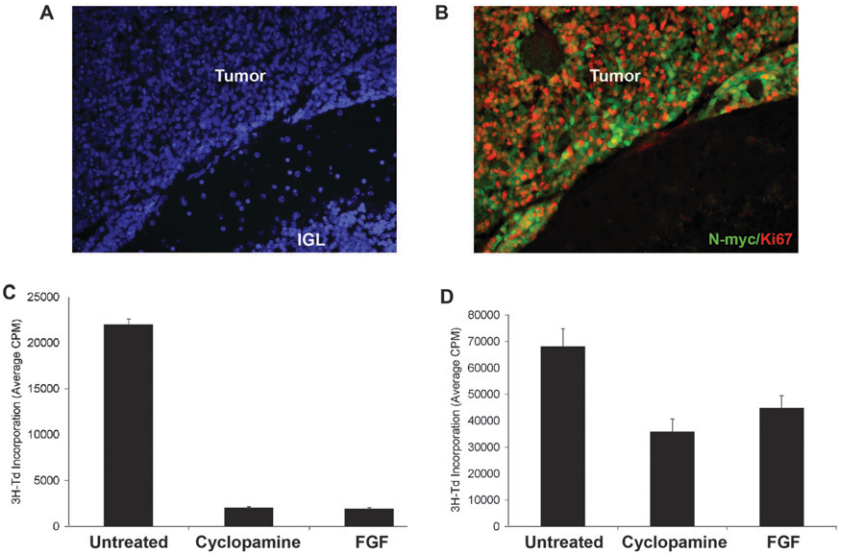

Figure 8. N-myc renders PNCs insensitive to hedgehog antagonists. (*A*,*B*) PNCs were infected with either GFP or N-myc encoding viruses for 24 h, and then cultured for an additional 24 h in the absence or presence of 3 μM cyclopamine prior to transplantation into the cerebellum of SCID-beige mice. Tumors developed in all animals transplanted with N-myc infected cells, whether or not they had been exposed to cyclopamine. (*A*,*B*) Sections of a tumor derived from N-myc-infected PNCs pretreated with cyclopamine, stained with DAPI (*A*) to label all nuclei or with antibodies against N-myc (green) and Ki67 (red) to detect proliferating tumor cells (*B*). Magnification, 20×. (*C*) Tumor cells from $ptc^{+/-}$ mice were cultured in the absence or presence of 1 μM cyclopamine or 25 ng/mL bFGF for 48 h, and then pulsed with ^{3}H-Td for an additional 18 h before being assayed for ^{3}H-Td incorporation. (*D*) Tumors resulting from transplantation of N-myc infected PNCs were harvested and FACS-sorted to purify infected (GFP^{+}) cells. These cells were cultured in the absence or presence of 1 μM cyclopamine or 25 ng/mL bFGF and analyzed as described above. Cyclopamine and bFGF markedly inhibited the growth of $ptc^{+/-}$ tumor cells but only modestly inhibited the growth of tumors derived from N-myc-infected PNCs (data in *C* and *D* are representative of five and three replicates, respectively).

and differentiating following transplantation into another animal is consistent with the existence of a cell-intrinsic differentiation program.

Our lineage-tracing studies also allowed us to test whether PNCs give rise to medulloblastoma. Although the presence of these cells in the cerebellum of animals that are destined to develop tumors has suggested that they represent the source of these tumors, it is also possible that PNCs simply represent persistent or ectopic GNPs (which have been observed in a number of other mutant mice) (Messer and Hatch 1984; Adams et al. 2002; Kerjan et al. 2005; Wiencken-Barger et al. 2007) and that tumors arise from a distinct population of progenitors. Indeed, a number of investigators have suggested that medulloblastomas, including those in $ptc^{+/-}$ mice, might arise from multipotent neural stem cells (Berman et al. 2002; Hemmati et al. 2003; Li et al. 2003; Singh et al. 2004). However, our fate-mapping studies demonstrate that tumors arise from cells that express Math1 between 4 and 6 wk of age. Since Math1 is expressed in lineage-restricted GNPs and PNCs and not in multipotent stem cells (Klein et al. 2005; Lee et al. 2005; Machold and Fishell 2005; Yang et al. 2008), these studies provide strong support for the notion that tumors in $ptc^{+/-}$ mice arise from PNCs.

Our demonstration that PNCs in $ptc^{+/-}$ mice give rise to medulloblastoma also has important implications for tumorigenesis in other tissues. Preneoplastic lesions have been identified in a number of tissues, including colon, breast, prostate, and pancreas (Levine and Ahnen 2006; Mokbel and Cutuli 2006; Montironi et al. 2007; Singh and Maitra 2007). In each case, these lesions contain proliferating cells with a morphology or organization distinct from that of normal tissue. While the lesions themselves do not meet the criteria for cancer, their presence is thought to predispose to cancer, and cancers are thought to arise from them. But while studies of human tissues are consistent with this view, there has been little direct evidence that preneoplastic lesions give rise to cancer. In fact, some studies have suggested that removal of polyps does not decrease the incidence of colon cancer, raising questions about whether these lesions actually give rise to tumors (Jass and Talbot 2001). Even in mouse models of cancer, there have been few studies linking preneoplastic lesions to end-stage tumors. For example, PNCs from mouse models of breast cancer (Maglione et al. 2001) and prostate cancer (Kim et al. 2002) can give rise to adenocarcinoma, but only after serial passaging of these cells in vivo. In contrast, we found that PNCs from $ptc^{+/-}$ mice can give rise to tumors without multiple passages. Together with our fate-mapping studies, these experiments provide the first direct evidence that preneoplastic lesions can give rise to tumors. The approaches we used should be readily adaptable to other systems in which there is a promoter that can be used to specifically label PNCs.

The fact that PNCs only rarely form tumors, either in situ or following transplantation, suggests that PNCs are not fully transformed and require additional mutations in order to form tumors. To test this hypothesis, we provided PNCs with a "second hit" by transducing them with N-myc retroviruses. Our studies demonstrated that N-myc caused a significant increase in the tumorigenic potential of PNCs, allowing them to generate tumors in 100% of recipients. The ability of N-myc to increase the incidence of medulloblastoma is consistent with several previous reports. First, amplification or overexpression of *N-myc* occurs in many cases of human medulloblastoma (Aldosari et al. 2002; Eberhart et al. 2002; Pomeroy et al.

2002) and in several mouse models of the disease (Shakhova et al. 2006; Yan et al. 2006; Frappart et al. 2007; Zindy et al. 2007), often in conjunction with mutation or deletion of *ptc*. Moreover, N-myc retroviruses cooperate with Shh retroviruses to transform GNPs in the neonatal cerebellum (Browd et al. 2006), and overexpression of N-myc in GNPs that lack p53 and Ink4c allows these cells to give rise to tumors in a transplantation assay (Zindy et al. 2007).

Interestingly, in many of these systems, N-myc overexpression alone was not sufficient to induce medulloblastoma. For example, in the retroviral transduction studies by Browd et al. (2006). N-myc viruses increased the frequency of tumors induced by Shh but could not induce tumors on their own. Likewise, in the transplantation studies by Zindy et al. (2007) mutation of *p53* and *ink4c* were required for tumors to form. Consistent with these findings, we observed that N-myc could not transform wild-type GNPs. The fact that N-myc is capable of inducing tumors in PNCs suggests that these cells have acquired changes that render them more sensitive to transformation. One such change is likely to be loss of *ptc* expression. However, previous work from our lab has identified a number of other genes whose expression is altered in PNCs compared with GNPs (Oliver et al. 2005), and it is possible that these genes may also contribute to the sensitivity of PNCs to transformation.

In considering how N-myc might promote tumorigenesis, we noted that PNCs that do not form tumors usually differentiate into granule neurons. This raised the possibility that N-myc might transform cells in part by inhibiting differentiation. Consistent with this possibility, we demonstrated that N-myc not only increased proliferation but also allowed cells to resist the differentiation-promoting effects of bFGF. Likewise, at a molecular level, N-myc not only induced expression of cyclin D1 but also promoted down-regulation of p27, critical regulators of differentiation in GNPs and medulloblastoma cells (Miyazawa et al. 2000; Knoepfler et al. 2002; Zindy et al. 2006). The transcriptional induction of cyclin D1 by N-myc may be a direct effect, as we and others have shown that overexpression of N-myc in GNPs increases cyclin D1 (Kenney and Rowitch 2000; Ciemerych et al. 2002; Kenney et al. 2003; Oliver et al. 2003). As for repression of p27, in neuroblastoma cells N-myc increases Cyclin E/cdk2 activity, which promotes phosphorylation of p27 and targets it for ubiquitination by the SCF complex (Nakamura et al. 2003). N-myc also increases expression of Skp-2, an F-box protein that can form part of the SCF complex (Bell et al. 2007). These events cooperate to promote ubiquitination and proteasome-dependent degradation of p27. Further studies will be necessary to determine whether N-myc promotes p27 degradation in this manner in PNCs. In any case, the dual capacity of N-myc to promote cell cycle progression and prevent differentiation appear to be key aspects of its transforming ability.

One of the most provocative findings of our study was the observation that N-myc can prevent differentiation and allow PNCs to form tumors even after exposure to cyclopamine. Previous studies showing cooperation between N-myc and Shh (Browd et al. 2006) have suggested that these two signals act synergistically to promote medulloblastoma formation, and that N-myc alone is not sufficient to initiate tumors. However, our demonstration that N-myc-infected PNCs become hedgehog pathway-independent suggests that the cooperation between these pathways may only be required during the early stages of tumorigenesis, and that once cells have become transformed by N-myc, the requirement for continued hedgehog signaling may be diminished. Many studies have shown that tumors initiated by overexpression of an oncogene or loss of a tumor suppressor become "addicted" to these mutations, implying that inhibition of the oncogene or restoration of the tumor suppressor might be effective approaches to therapy (Jain et al. 2002; Fleming et al. 2005; Martins et al. 2006; Sharma and Settleman 2007). The insensitivity of N-myc-expressing PNCs to hedgehog antagonists argues that tumors initiated by mutations in the hedgehog pathway may not necessarily remain addicted to this pathway. Similar findings have been reported recently for c-myc-induced lung and mammary tumors (Boxer et al. 2004; Tran et al. 2008).

The possibility that N-myc overexpression can render tumors resistant to hedgehog antagonists has important clinical implications. N-myc amplification and hedgehog pathway mutations are both relatively common events in human medulloblastoma. Although the frequency with which these events coincide is unknown, tumors bearing hedgehog pathway mutations have been shown to express high levels of N-myc RNA (Pomeroy et al. 2002; Thompson et al. 2006). If overexpression of N-myc renders mouse medulloblastoma cells insensitive to hedgehog pathway antagonists, it might have a similar effect in human tumors. With hedgehog antagonists moving toward clinical trials for medulloblastoma and other types of cancer (Romer and Curran 2005; Epstein 2008), it is important to consider the possibility that some tumors that are initially dependent on hedgehog signaling may acquire secondary mutations that render them insensitive to these agents.

In summary, we demonstrated that PNCs in $ptc^{+/-}$ mice represent a unique population of cells that is poised on the precipice of malignancy. While the majority of PNCs proliferate only transiently and then undergo differentiation and migration, a subset of these cells continues to divide and ultimately gives rise to tumors. But even PNCs that do not normally form tumors have the capacity to do so with the introduction of a single oncogenic lesion. Further studies of these cells, and the genes that regulate their fate, will shed light on the molecular etiology of medulloblastoma.

Materials and methods

Animals

$ptc^{+/-}$ mice (Goodrich et al. 1997) were maintained by crossing with 129X1/SvJ mice (Jackson Laboratories). Math1-GFP mice

were obtained from Jane Johnson at University of Texas Southwestern Medical Center. Math1-GFP/*ptc*$^{+/-}$ (M-ptc) mice were generated and maintained as described previously (Oliver et al. 2005). Cre-inducible AP reporter mice (R26R-hPLAP) were generated by first cloning a 2.0-kb EcoRI–XhoI fragment of the *hPLAP* cDNA (Leighton et al. 2001) into the pBigT plasmid (Srinivas et al. 2001) immediately after the loxP-neo-4xpoly A-loxP cassette. The 5.2-kb PacI–AscI fragment containing loxP-neo-4xpolyA-loxP-hPLAP-polyA (STOP-hPLAP) was then inserted into a R26R-acceptor plasmid (Srinivas et al. 2001). A 1.6-kb chicken *actin* (CAG) promoter was then cloned into the PacI site upstream of the STOP-hPLAP cassette. This targeting construct was electroporated into embryonic stem (ES) cells and Rosa-CAG-STOP-hPLAP knock-in mice were generated from targeted ES cell clones. Math1-CreER^{T2} mice (Machold and Fishell 2005) were generously provided by Gord Fishell at New York University. MAP mice were generated by mating Math1-CreER^{T2} mice with *ptc*$^{+/-}$ mice, and then crossing the resulting double transgenics with R26R-hPLAP mice to generate triple transgenic mice. All mice were bred and maintained in the Cancer Center Isolation Facility at Duke University.

In vivo labeling of GNPs and PNCs

Tamoxifen (Sigma) was prepared as a 20 mg/mL stock solution in corn oil (Sigma). For P8 labeling, Math1-CreER/R26R-hPLAP pups received 30 μL of tamoxifen stock solution by oral gavage. For PNC and tumor cell labeling, MAP mice were orally gavaged with 200 μL of tamoxifen stock solution.

Tissue preparation, cryosectioning, and staining

Mice were perfused with PBS and 4% paraformaldehyde (PFA) in PBS to fix all tissues. Cerebella were harvested and fixed in 4% PFA overnight at 4°C and then cryoprotected in 30% sucrose solution. Tissues were embedded in Tissue-Tek OCT (Sakura Finetech). Cerebella were cut into 12-μM sections using a Leica 3050S cryostat (Vashaw Scientific).

For hematoxylin and eosoin (H&E) staining, slides were dipped in Harris' Hematoxylin (Sigma) for 5 min, cleared in running tap water for 5 min, and destained in acid alcohol. Slides were then "blued" in 0.05% lithium carbonate, washed in dH_2O, and stained in 50% Eosin (Sigma). After dehydration in ethanol, slides were permanently mounted in VectaMount (Vector Laboratories).

AP staining of MAP cerebella was performed by fixing sections for 1 h at room temperature in 4% PFA. Endogenous AP was heat-inactivated by incubating slides in PBS for 3 h at 65°C. Slides were washed in a solution of 100 mM NaCl and 100 mM Tris-HCl (pH 7.5), and then incubated for 1 h at 37°C with the AP substrate NBT/BCIP (Roche) diluted 1:50 in staining buffer (100 mM Tris-Hcl at pH 9.5, 100 mM NaCl, 5 mM $MgCl_2$). The reaction was stopped in PBS and slides were mounted in Aqua-polymount (Polysciences, Inc.).

Immunofluorescence (IF) staining was performed as follows: Tissue sections or cells were rehydrated in PBS with 0.1% TritonX-100 (PBST) for 10 min. Slides were then blocked in PBST + 10% normal goat serum (Jackson ImmunoResearch) for 1 h at room temperature. Sections were incubated overnight at 4°C in primary antibodies diluted in immunostaining buffer (PBST + 2% BSA). Slides were washed and then incubated with secondary antibodies for 1 h at room temperature. Nuclei were stained with DAPI (Invitrogen) and slides were mounted in Fluoromount-G (Southern Biotech). Images were taken using a Leica AxioImager (Leica Microsystems) and Metamorph Software (Molecular Devices). Antibodies used for IF included Ki67 (1:100, BD Biosciences), NeuN (1:100; Chemicon), Gabra6 (1:200; Chemicon), β−gal (1:600; Promega), GFP (1:100; Invitrogen), N-myc (1:100; Calbiochem), cleaved caspase-3 (1:300; Cell Signaling), and p27 (1:100; BD Biosciences).

Double AP/IF staining was performed using the fluorescent AP substrate Fast Red (Roche). Tissues were fixed and heat-inactivated for 3 h at 65°C as described above, and then stained with primary and secondary antibodies. Slides were then washed in 100 mM Tris-HCl (pH 8), 100 mM NaCl, 10 mM $MgCl_2$, and incubated in Fast Red solution (2 mL 0.1 M Tris-Hcl at pH 8.2 per tablet) for 1–4 h at room temperature. After staining, slides were washed in 100 mM Tris-HCl (pH 7.5), 150 mM NaCl, and 0.05% Tween-20, and counterstained with DAPI as above. Slides were mounted in VectaShield (Vector Laboratories).

X-gal staining was performed by permeabilizing sections in 0.01% deoxycholate, washing in PBS, and incubating in X-gal staining solution (0.4 mg/mL X-gal, 10 mM potassium ferrocyanide, 10 mM potassium ferricyanide, 1 mM $MgCl_2$) overnight at 37°C.

TUNEL staining was performed using the In Situ Cell Death Detection Kit, POD (Roche). Briefly, slides were fixed in 4% PFA for 20 min, washed in PBS, and permeabilized in 0.1% Triton X-100 + 0.1% sodium citrate. To reduce background, slides were blocked in PBS + 2% BSA for 30 min. The slides were then incubated in TUNEL labeling reaction mix for 1 h at 37°C. After termination of the labeling, sections were counterstained with DAPI and mounted using Fluoromount G. Labeled cells were visualized using a Leica AxioImager and Metamorph software.

Preneoplastic lesion quantitation and analysis

Cerebella from 6 and 12-wk-old M-ptc mice were harvested as described above. The entire cerebellum from each animal was serially sectioned. To identify PNCs for each cerebellum, every fifth slide (12–14 slides per cerebellum) was stained with DAPI. Images of the lesions were taken on either the Leica AxioImager or a Zeiss 510 inverted scanning confocal microscope. All images were taken at 10× magnification and calibrated using Metamorph image software. To determine area, the preneoplastic lesion was defined in Metamorph and area was calculated based on the micromolar per pixel calibration. To calculate volume, the average area of the preneoplastic lesion was multiplied by the section thickness (12 μM) and the number of sections in which the lesion was observed.

Laser capture microdissection

Cerebella from wild-type P7 and 5- to 6-wk-old M-ptc mice were frozen (without prior fixation) in OCT and sectioned as described above at 10-μm thickness. Sections were stained and dehydrated using the Molecular Devices HistoGene LCM Frozen Section Staining Kit (Molecular Devices). Cells were captured using the Arcturus Laser Capture Microsdissection system (Molecular Devices). RNA was isolated using the PicoPure RNA isolation kit (Molecular Devices).

Isolation and retroviral infection of PNCs and tumor cells

PNCs were isolated from 5- to 6-wk-old *ptc*$^{+/-}$ mice, and tumor cells were isolated from 3- to 6-mo-old *ptc*$^{+/-}$ mice with signs of medulloblastoma, as described previously (Oliver et al. 2005). Cells were plated on poly-D-lysine-coated tissue culture dishes in Neurobasal medium containing B27 supplement, sodium pyruvate, L-glutamine, and penicillin/streptomycin (NB-B27; all components from Invitrogen). Immediately after isolation, cells were infected with supernatants from 293T cells transfected

with gag-pol and VSV-G plasmids and either control GFP retroviral vectors (MSCV-IRES-GFP or LZRS-IRES-GFP) or vectors encoding N-myc (LZRS-N-myc-IRES-GFP). Cells were cultured with virus for 24 h prior to harvesting for transplantation.

Intracerebellar transplantation

For transplantation of naive PNCs and tumor cells, freshly isolated cells were resuspended in NB-B27 at a concentration of 1×10^5 cells per microliter. For retroviral overexpression experiments, infected cells were removed from the culture dish by digestion with papain (Worthington Biochemical), washed, and resuspended in NB-B27 at a concentration of 1×10^5 cells per microliter. SCID-beige hosts (4–6 wk old; Taconic Farms) were used for these transplants because the heterogeneous genetic background of the $ptc^{+/-}$ mice precludes transplantation into syngeneic hosts. SCID-beige animals were anesthetized by intraperitoneal injection with 100 mg/kg ketamine (Fort Dodge Animal Health) + 9 mg/kg xylazine (Ben Venure Laboratories). Once anesthetized, the fur was shaved from the head and the scalp prepared with ethanol and betadine scrubs. The animal was positioned in a Kopf stereotaxic frame with a mouse adaptor (Kopf Instruments), and a 0.5-inch incision was made in the skin from the top of the skull to just below the ears. A beveled end 18-G needle was used to bore a hole directly above the cerebellum. An unbeveled 24-gauge Hamilton syringe, loaded with 5 μL of the cell suspension and mounted in a micromanipulator, was inserted into the hole at a depth of 1 mm. The cells were injected slowly, the syringe was removed, and the incision was treated with one to two drops of 0.25% bupivicaine (post-operative analgesic; Hospira), and sutured using 6-0 fast-absorbing plaint gut suture on a 3/8 PC-1 cutting needle (Ethicon) and the animals were then allowed to recover. Animals were monitored for symptoms of medulloblastoma for 4–6 mo post-transplantation.

Proliferation assays

Cells were cultured in poly(d-lysine)-coated 96-well plates at 2×10^5 cells per well. For infection/treatment experiments, PNCs were infected for 24 h prior to addition of either bFGF (25 ngl/mL; Peprotech) or cyclopamine (1 uM; Toronto Research Chemicals). After 48 h, cells were pulsed with [methyl-^{3}H]thymidine (GE Healthcare). After 16 h, cells were harvested by using a Mach IIIM Manual Harvester 96 (TOMTEC), and incorporated radioactivity was quantitated by using a Wallac MicroBeta microplate scintillation counter (PerkinElmer).

RNA isolation, cDNA synthesis, and real-time RT–PCR

mRNA was isolated from cells and tissue using the Qiagen RNAeasy kit (Qiagen) and treated with DNA-free DNase treatment and removal reagents (Ambion). cDNA was synthesized using oligo(dT) and SuperscriptII RT (Invitrogen). Real-Time RT–PCR reactions were performed in triplicate on the cDNA using Bio-Rad iQ SYBR green supermix and the Bio-Rad iQ5 Multicolor Real-Time PCR Detection System (Bio-Rad). Mouse primers used for real-time RT–PCR included *β-2-microglobulin*, *gli1*, *cyclin D1*, *math1*, and wild-type *patched*.

Acknowledgments

We thank Sam Johnson and the Duke Light Microscopy Core Facility for assistance with microscopy, Bob Weinberg for helpful advice and insight, Simon Gregory for use of the Laser Capture Microdissection system, and Tracy-Ann Read for assistance with transplantation. This work was supported by funding from the National Cancer Center (J.D.K.), NIDCR grant #DE016550 (F.W), the Whitehall Foundation (F.W), the McKnight Endowment Fund for Neuroscience (F.W), the Japanese Society for the Promotion of Science (H.H), the Children's Brain Tumor Foundation (R.W.R.), the McDonnell Foundation (R.W.R.), the Pediatric Brain Tumor Foundation of the US (R.W.R.), and NINDS grant #NS-052323-01 (R.W.R.).

References

Adams, N.C., Tomoda, T., Cooper, M., Dietz, G., and Hatten, M.E. 2002. Mice that lack astrotactin have slowed neuronal migration. *Development* **129:** 965–972.

Aldosari, N., Bigner, S.H., Burger, P.C., Becker, L., Kepner, J.L., Friedman, H.S., and McLendon, R.E. 2002. MYCC and MYCN oncogene amplification in medulloblastoma. A fluorescence in situ hybridization study on paraffin sections from the Children's Oncology Group. *Arch. Pathol. Lab. Med.* **126:** 540–544.

Bell, E., Lunec, J., and Tweddle, D.A. 2007. Cell cycle regulation targets of MYCN identified by gene expression microarrays. *Cell Cycle* **6:** 1249–1256.

Ben-Arie, N., Hassan, B.A., Bermingham, N.A., Malicki, D.M., Armstrong, D., Matzuk, M., Bellen, H.J., and Zoghbi, H.Y. 2000. Functional conservation of atonal and Math1 in the CNS and PNS. *Development* **127:** 1039–1048.

Berman, D.M., Karhadkar, S.S., Hallahan, A.R., Pritchard, J.I., Eberhart, C.G., Watkins, D.N., Chen, J.K., Cooper, M.K., Taipale, J., Olson, J.M., et al. 2002. Medulloblastoma growth inhibition by hedgehog pathway blockade. *Science* **297:** 1559–1561.

Boxer, R.B., Jang, J.W., Sintasath, L., and Chodosh, L.A. 2004. Lack of sustained regression of c-MYC-induced mammary adenocarcinomas following brief or prolonged MYC inactivation. *Cancer Cell* **6:** 577–586.

Browd, S.R., Kenney, A.M., Gottfried, O.N., Yoon, J.W., Walterhouse, D., Pedone, C.A., and Fults, D.W. 2006. N-myc can substitute for insulin-like growth factor signaling in a mouse model of sonic hedgehog-induced medulloblastoma. *Cancer Res.* **66:** 2666–2672.

Ciemerych, M.A., Kenney, A.M., Sicinska, E., Kalaszczynska, I., Bronson, R.T., Rowitch, D.H., Gardner, H., and Sicinski, P. 2002. Development of mice expressing a single D-type cyclin. *Genes & Dev.* **16:** 3277–3289.

Dahmane, N. and Ruiz-i-Altaba, A. 1999. Sonic hedgehog regulates the growth and patterning of the cerebellum. *Development* **126:** 3089–3100.

Dellovade, T., Romer, J.T., Curran, T., and Rubin, L.L. 2006. The hedgehog pathway and neurological disorders. *Annu. Rev. Neurosci.* **29:** 539–563.

Eberhart, C.G., Kratz, J.E., Schuster, A., Goldthwaite, P., Cohen, K.J., Perlman, E.J., and Burger, P.C. 2002. Comparative genomic hybridization detects an increased number of chromosomal alterations in large cell/anaplastic medulloblastomas. *Brain Pathol.* **12:** 36–44.

Epstein, E.H. 2008. Basal cell carcinomas: Attack of the hedgehog. *Nature Reviews* **8:** 743–754.

Fleming, J.B., Shen, G.L., Holloway, S.E., Davis, M., and Brekken, R.A. 2005. Molecular consequences of silencing mutant K-ras in pancreatic cancer cells: Justification for K-ras-directed therapy. *Mol. Cancer Res.* **3:** 413–423.

Fogarty, M.P., Kessler, J.D., and Wechsler-Reya, R.J. 2005. Morphing into cancer: The role of developmental signaling pathways in brain tumor formation. *J. Neurobiol.* **64:** 458–475.

Fogarty, M.P., Emmenegger, B.A., Grasfeder, L.L., Oliver, T.G., and Wechsler-Reya, R.J. 2007. Fibroblast growth factor blocks Sonic hedgehog signaling in neuronal precursors and tumor cells. *Proc. Natl. Acad. Sci.* **104:** 2973–2978.

Frappart, P.O., Lee, Y., Lamont, J., and McKinnon, P.J. 2007. BRCA2 is required for neurogenesis and suppression of medulloblastoma. *EMBO J.* **26:** 2732–2742.

Goodrich, L.V., Milenkovic, L., Higgins, K.M., and Scott, M.P. 1997. Altered neural cell fates and medulloblastoma in mouse *patched* mutants. *Science* **277:** 1109–1113.

Hallahan, A.R., Pritchard, J.I., Hansen, S., Benson, M., Stoeck, J., Hatton, B.A., Russell, T.L., Ellenbogen, R.G., Bernstein, I.D., Beachy, P.A., et al. 2004. The SmoA1 mouse model reveals that notch signaling is critical for the growth and survival of sonic hedgehog-induced medulloblastomas. *Cancer Res.* **64:** 7794–7800.

Hanahan, D. and Weinberg, R.A. 2000. The hallmarks of cancer. *Cell* **100:** 57–70.

Hemmati, H.D., Nakano, I., Lazareff, J.A., Masterman-Smith, M., Geschwind, D.H., Bronner-Fraser, M., and Kornblum, H.I. 2003. Cancerous stem cells can arise from pediatric brain tumors. *Proc. Natl. Acad. Sci.* **100:** 15178–15183.

Jain, M., Arvanitis, C., Chu, K., Dewey, W., Leonhardt, E., Trinh, M., Sundberg, C.D., Bishop, J.M., and Felsher, D.W. 2002. Sustained loss of a neoplastic phenotype by brief inactivation of MYC. *Science* **297:** 102–104.

Jass, J.R. and Talbot, I.C. 2001. Molecular and cellular biology of pre-malignancy in the gastrointestinal tract. *Best Pract. Res. Clin. Gastroenterol.* **15:** 175–189.

Jia, J. and Jiang, J. 2006. Decoding the Hedgehog signal in animal development. *Cell. Mol. Life Sci.* **63:** 1249–1265.

Kenney, A.M. and Rowitch, D.H. 2000. Sonic hedgehog promotes G(1) cyclin expression and sustained cell cycle progression in mammalian neuronal precursors. *Mol. Cell. Biol.* **20:** 9055–9067.

Kenney, A.M., Cole, M.D., and Rowitch, D.H. 2003. Nmyc upregulation by sonic hedgehog signaling promotes proliferation in developing cerebellar granule neuron precursors. *Development* **130:** 15–28.

Kerjan, G., Dolan, J., Haumaitre, C., Schneider-Maunoury, S., Fujisawa, H., Mitchell, K.J., and Chedotal, A. 2005. The transmembrane semaphorin Sema6A controls cerebellar granule cell migration. *Nat. Neurosci.* **8:** 1516–1524.

Kim, M.J., Bhatia-Gaur, R., Banach-Petrosky, W.A., Desai, N., Wang, Y., Hayward, S.W., Cunha, G.R., Cardiff, R.D., Shen, M.M., and Abate-Shen, C. 2002. Nkx3.1 mutant mice recapitulate early stages of prostate carcinogenesis. *Cancer Res.* **62:** 2999–3004.

Kim, J.Y., Nelson, A.L., Algon, S.A., Graves, O., Sturla, L.M., Goumnerova, L.C., Rowitch, D.H., Segal, R.A., and Pomeroy, S.L. 2003. Medulloblastoma tumorigenesis diverges from cerebellar granule cell differentiation in patched heterozygous mice. *Dev. Biol.* **263:** 50–66.

Klein, C., Butt, S.J., Machold, R.P., Johnson, J.E., and Fishell, G. 2005. Cerebellum- and forebrain-derived stem cells possess intrinsic regional character. *Development* **132:** 4497–4508.

Knoepfler, P.S., Cheng, P.F., and Eisenman, R.N. 2002. N-myc is essential during neurogenesis for the rapid expansion of progenitor cell populations and the inhibition of neuronal differentiation. *Genes & Dev.* **16:** 2699–2712.

Lee, Y., Miller, H.L., Jensen, P., Hernan, R., Connelly, M., Wetmore, C., Zindy, F., Roussel, M.F., Curran, T., Gilbertson, R.J., et al. 2003. A molecular fingerprint for medulloblastoma. *Cancer Res.* **63:** 5428–5437.

Lee, A., Kessler, J.D., Read, T.A., Kaiser, C., Corbeil, D., Huttner, W.B., Johnson, J.E., and Wechsler-Reya, R.J. 2005. Isolation of neural stem cells from the postnatal cerebellum. *Nat. Neurosci.* **8:** 723–729.

Leighton, P.A., Mitchell, K.J., Goodrich, L.V., Lu, X., Pinson, K., Scherz, P., Skarnes, W.C., and Tessier-Lavigne, M. 2001. Defining brain wiring patterns and mechanisms through gene trapping in mice. *Nature* **410:** 174–179.

Levine, J.S. and Ahnen, D.J. 2006. Clinical practice. Adenomatous polyps of the colon. *N. Engl. J. Med.* **355:** 2551–2557.

Li, L., Connelly, M.C., Wetmore, C., Curran, T., and Morgan, J.I. 2003. Mouse embryos cloned from brain tumors. *Cancer Res.* **63:** 2733–2736.

Lum, L. and Beachy, P.A. 2004. The Hedgehog response network: Sensors, switches, and routers. *Science* **304:** 1755–1759.

Lumpkin, E.A., Collisson, T., Parab, P., Omer-Abdalla, A., Haeberle, H., Chen, P., Doetzlhofer, A., White, P., Groves, A., Segil, N., et al. 2003. Math1-driven GFP expression in the developing nervous system of transgenic mice. *Gene Expr. Patterns* **3:** 389–395.

Machold, R. and Fishell, G. 2005. Math1 is expressed in temporally discrete pools of cerebellar rhombic-lip neural progenitors. *Neuron* **48:** 17–24.

Maglione, J.E., Moghanaki, D., Young, L.J., Manner, C.K., Ellies, L.G., Joseph, S.O., Nicholson, B., Cardiff, R.D., and MacLeod, C.L. 2001. Transgenic Polyoma middle-T mice model premalignant mammary disease. *Cancer Res.* **61:** 8298–8305.

Martins, C.P., Brown-Swigart, L., and Evan, G.I. 2006. Modeling the therapeutic efficacy of p53 restoration in tumors. *Cell* **127:** 1323–1334.

Messer, A. and Hatch, K. 1984. Persistence of cerebellar thymidine kinase in staggerer and hypothyroid mutants. *J. Neurogenet.* **1:** 239–248.

Miyazawa, K., Himi, T., Garcia, V., Yamagishi, H., Sato, S., and Ishizaki, Y. 2000. A role for p27/Kip1 in the control of cerebellar granule cell precursor proliferation. *J. Neurosci.* **20:** 5756–5763.

Mokbel, K. and Cutuli, B. 2006. Heterogeneity of ductal carcinoma in situ and its effects on management. *Lancet Oncol.* **7:** 756–765.

Montironi, R., Mazzucchelli, R., Lopez-Beltran, A., Cheng, L., and Scarpelli, M. 2007. Mechanisms of disease: High-grade prostatic intraepithelial neoplasia and other proposed preneoplastic lesions in the prostate. *Nat. Clin. Pract. Urol.* **4:** 321–332.

Nakamura, M., Matsuo, T., Stauffer, J., Neckers, L., and Thiele, C.J. 2003. Retinoic acid decreases targeting of p27 for degradation via an N-myc-dependent decrease in p27 phosphorylation and an N-myc-independent decrease in Skp2. *Cell Death Differ.* **10:** 230–239.

Nicot, A., Lelievre, V., Tam, J., Waschek, J.A., and DiCicco-Bloom, E. 2002. Pituitary adenylate cyclase-activating polypeptide and sonic hedgehog interact to control cerebellar granule precursor cell proliferation. *J. Neurosci.* **22:** 9244–9254.

Oliver, T.G., Grasfeder, L.L., Carroll, A.L., Kaiser, C., Gillingham, C.L., Lin, S.M., Wickramasinghe, R., Scott, M.P., and Wechsler-Reya, R.J. 2003. Transcriptional profiling of the Sonic hedgehog response: A critical role for N-myc in proliferation of neuronal precursors. *Proc. Natl. Acad. Sci.* **100:** 7331–7336.

Oliver, T.G., Read, T.A., Kessler, J.D., Mehmeti, A., Wells, J.F., Huynh, T.T., Lin, S.M., and Wechsler-Reya, R.J. 2005. Loss of patched and disruption of granule cell development in a preneoplastic stage of medulloblastoma. *Development* **132:** 2425–2439.

Pomeroy, S.L., Tamayo, P., Gaasenbeek, M., Sturla, L.M., Angelo, M., McLaughlin, M.E., Kim, J.Y., Goumnerova, L.C., Black, P.M., Lau, C., et al. 2002. Prediction of central

nervous system embryonal tumour outcome based on gene expression. *Nature* **415:** 436–442.
Rohatgi, R. and Scott, M.P. 2007. Patching the gaps in Hedgehog signalling. *Nat. Cell Biol.* **9:** 1005–1009.
Romer, J. and Curran, T. 2005. Targeting medulloblastoma: Small-molecule inhibitors of the Sonic Hedgehog pathway as potential cancer therapeutics. *Cancer Res.* **65:** 4975–4978.
Sanchez, P. and Ruiz i Altaba, A. 2005. In vivo inhibition of endogenous brain tumors through systemic interference of Hedgehog signaling in mice. *Mech. Dev.* **122:** 223–230.
Sasai, K., Romer, J.T., Lee, Y., Finkelstein, D., Fuller, C., McKinnon, P.J., and Curran, T. 2006. Shh pathway activity is down-regulated in cultured medulloblastoma cells: Implications for preclinical studies. *Cancer Res.* **66:** 4215–4222.
Shakhova, O., Leung, C., van Montfort, E., Berns, A., and Marino, S. 2006. Lack of Rb and p53 delays cerebellar development and predisposes to large cell anaplastic medulloblastoma through amplification of N-Myc and Ptch2. *Cancer Res.* **66:** 5190–5200.
Sharma, S.V. and Settleman, J. 2007. Oncogene addiction: Setting the stage for molecularly targeted cancer therapy. *Genes & Dev.* **21:** 3214–3231.
Singh, M. and Maitra, A. 2007. Precursor lesions of pancreatic cancer: Molecular pathology and clinical implications. *Pancreatology* **7:** 9–19.
Singh, S.K., Hawkins, C., Clarke, I.D., Squire, J.A., Bayani, J., Hide, T., Henkelman, R.M., Cusimano, M.D., and Dirks, P.B. 2004. Identification of human brain tumour initiating cells. *Nature* **432:** 396–401.
Srinivas, S., Watanabe, T., Lin, C.S., William, C.M., Tanabe, Y., Jessell, T.M., and Costantini, F. 2001. Cre reporter strains produced by targeted insertion of EYFP and ECFP into the ROSA26 locus. *BMC Dev. Biol.* **1:** 4. doi:10.1186/1471-213X-1-4.
Thompson, M.C., Fuller, C., Hogg, T.L., Dalton, J., Finkelstein, D., Lau, C.C., Chintagumpala, M., Adesina, A., Ashley, D.M., Kellie, S.J., et al. 2006. Genomics identifies medulloblastoma subgroups that are enriched for specific genetic alterations. *J. Clin. Oncol.* **24:** 1924–1931.
Tran, P.T., Fan, A.C., Bendapudi, P.K., Koh, S., Komatsubara, K., Chen, J., Horng, G., Bellovin, D.I., Giuriato, S., Wang, C.S., et al. 2008. Combined Inactivation of MYC and K-Ras oncogenes reverses tumorigenesis in lung adenocarcinomas and lymphomas. *PLoS One* **3:** e2125. doi:10.1371/journal.pone.0002125.
Uziel, T., Zindy, F., Xie, S., Lee, Y., Forget, A., Magdaleno, S., Rehg, J.E., Calabrese, C., Solecki, D., Eberhart, C.G., et al. 2005. The tumor suppressors Ink4c and p53 collaborate independently with Patched to suppress medulloblastoma formation. *Genes & Dev.* **19:** 2656–2667.
Wallace, V.A. 1999. Purkinje-cell-derived Sonic hedgehog regulates granule neuron precursor cell proliferation in the developing mouse cerebellum. *Curr. Biol.* **9:** 445–448.
Wechsler-Reya, R.J. and Scott, M.P. 1999. Control of neuronal precursor proliferation in the cerebellum by Sonic Hedgehog [see comments]. *Neuron* **22:** 103–114.
Wetmore, C., Eberhart, D.E., and Curran, T. 2000. The normal patched allele is expressed in medulloblastomas from mice with heterozygous germ-line mutation of patched. *Cancer Res.* **60:** 2239–2246.
Wiencken-Barger, A.E., Djukic, B., Casper, K.B., and McCarthy, K.D. 2007. A role for Connexin43 during neurodevelopment. *Glia* **55:** 675–686.
Yan, C.T., Kaushal, D., Murphy, M., Zhang, Y., Datta, A., Chen, C., Monroe, B., Mostoslavsky, G., Coakley, K., Gao, Y., et al. 2006. XRCC4 suppresses medulloblastomas with recurrent translocations in p53-deficient mice. *Proc. Natl. Acad. Sci.* **103:** 7378–7383.
Yang, Z.J., Ellis, T., Markant, S.L., Read, T.A., Kessler, J.D., Bourboulas, M., Schuller, U., Machold, R., Fishell, G., Rowitch, D.H., et al. 2008. Medulloblastoma can be initiated by deletion of Patched in lineage-restricted progenitors or stem cells. *Cancer Cell* **14:** 135–145.
Zhao, H., Ayrault, O., Zindy, F., Kim, J.H., and Roussel, M.F. 2008. Post-transcriptional down-regulation of Atoh1/Math1 by bone morphogenic proteins suppresses medulloblastoma development. *Genes & Dev.* **22:** 722–727.
Zindy, F., Knoepfler, P.S., Xie, S., Sherr, C.J., Eisenman, R.N., and Roussel, M.F. 2006. N-Myc and the cyclin-dependent kinase inhibitors p18Ink4c and p27Kip1 coordinately regulate cerebellar development. *Proc. Natl. Acad. Sci.* **103:** 11579–11583.
Zindy, F., Uziel, T., Ayrault, O., Calabrese, C., Valentine, M., Rehg, J.E., Gilbertson, R.J., Sherr, C.J., and Roussel, M.F. 2007. Genetic alterations in mouse medulloblastomas and generation of tumors de novo from primary cerebellar granule neuron precursors. *Cancer Res.* **67:** 2676–2684.